Growth Model for Atomic Ordering: The Case for Quadruple-Period Ordering in GaAsSb Alloys

Iskander G. Batyrev, Andrew G. Norman, S. B. Zhang, and Su-Huai Wei
National Renewable Energy Laboratory, Golden, Colorado 80401
(Received 3 June 2002; published 15 January 2003)

Quadruple-period ordering in GaAsSb alloys is studied both theoretically and experimentally. A growth model is proposed to account for the observed three-dimensional (3D) ordered structure. The model is qualitatively different from the widely accepted surface reconstruction and dimerization-induced ordering models that strictly speaking explain only the in-plane 2D patterns. Here, we show that the already ordered substrate will affect the reconstruction of the growth front with respect to the substrate to ensure a correct stacking of the individual 2D ordered layers into the observed 3D lattice.

DOI: 10.1103/PhysRevLett.90.026102 PACS numbers: 68.35.–p, 68.37.–d, 68.55.Ac

It has long been understood that atomic ordering, widely observed in epitaxially grown semiconductor AB_xC_{1-x} alloys, is driven by surface thermodynamics and/or by growth kinetics, but not by bulk thermodynamics [1]. Not only that, the observed ordered phases often have a higher energy than either the disordered alloy or other yet-to-be observed ordered structures [2]. Atomic dimerization and reconstruction at the growing surface, typically a (001) surface, naturally provides an atomic-scale compressive/tensile strain field below the surface [3,4]. This creates a subsurface site preference for size-mismatched B and C atoms and hence ordering [4,5]. This dimerization-induced ordering view is widely held but, strictly speaking, describes only a two-dimensional (2D) phenomenon. In order to obtain the observed three-dimensional (3D) ordering pattern, the 2D layers have to be adequately stacked. It is customary to invoke surface steps to complete the 3D ordering, as several experiments have correlated the degree of ordering with the density and orientation of surface steps [6–8]. However, a microscopic model regarding step-induced 3D stacking based on first-principles theory is still lacking. Recently, surface induced 2D ordering of nanoclusters was also observed, extending the study of the atomic ordering phenomenon into nanosciences [9].

Recently, a new quadruple-period (QP) ordering was observed in $GaAs_{1-x}Sb_x$ alloys ($0.05 < x < 0.2$) by transmission electron diffraction (TED) [10] and x-ray diffraction measurements [11]. Figure 1(a) shows a $(\bar{1}10)$ cross-section TED pattern of a $GaAs_{0.89}Sb_{0.11}$ film grown by molecular beam epitaxy (MBE) at 625 °C. Kinematical diffraction calculations reveal that the ordered structure in Fig. 1(b) gives the TED pattern [Fig. 1(c)] that best matches the experiment [Fig. 1(a)]. The QP ordered structure has several extraordinary but unexplained physical features such as the following.

(i) The growth of the quadruple-period ordered materials requires a high growth temperature ($T > 600$ °C). At such temperatures, although the 2×4 surface pattern still holds, the surface transforms into a different reconstruction, as seen by reflection high energy electron diffraction (RHEED).

(ii) It has a CuAu-like structure *but* with a periodic array of antiphase boundaries along the [110] direction. Although similar antiphase superlattices have been observed previously in metal alloys [12] this is the first report of such a structure in a semiconductor alloy.

(iii) The ordering direction is perpendicular to the surface anion dimer direction. Hence, even within the framework of surface-dimerization induced 2D ordering, it is still not clear why such an ordering would have taken place at all, unless it is associated with surface cation dimers.

(iv) To our knowledge, the quadruple period of 1.6 nm represents the longest period in 3D atomic ordering in semiconductor alloys observed so far. Hence, an understanding of the QP ordering may provide the crucial insights on how to fabricate artificial 3D lattices out of already existing 2D nanostructure arrays [9].

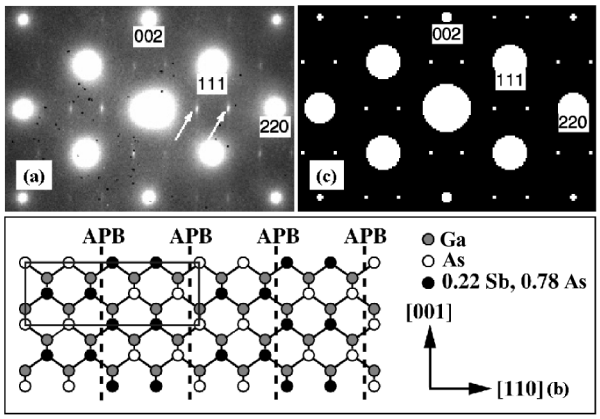

FIG. 1. (a) The $(\bar{1}10)$ cross-section TED pattern of the MBE $GaAs_{0.89}Sb_{0.11}$ layer grown at 625 °C. It contains pairs of superlattice spots (e.g., arrowed) arising from a quadruple-period ordering along [110]. (b) The $[\bar{1}10]$ projection of the ordered structure. (c) The calculated TED pattern for the structure in (b).

In this paper, we combine first-principles total energy calculations with experimental analyses to determine the atomic structure of the QP ordering in $GaAs_{1-x}Sb_x$ alloys and the ordering mechanism. A close relationship between a high-temperature Sb-stabilized (001)-$\delta_2(2 \times 4)$ surface reconstruction and the QP ordering is established. We propose that an interplay between the already grown substrate and the reconstructed surface at the growth front could be a general missing link between 2D and 3D ordering in semiconductor alloys. In other words, although the surface reconstruction has been established by the growth conditions, there are still remaining degrees of freedom regarding translation and flip-flop of the surface structure with respect to the substrate (see below). This leaves room for the development, via surface energetics, of the final 3D patterns seen by experiments. Our calculations on the $GaAs_{0.5}Sb_{0.5}$ alloy explain the formation of periodic antiphase boundaries and hence the observed quadruple-period ordering.

$GaAs_{0.89}Sb_{0.11}$ films have been grown by MBE at 625 °C on semi-insulating GaAs (001) substrates. The surface reconstruction during the growth is 2×4 as determined by *in situ* RHEED. Layer compositions were measured using x-ray diffraction. The atomic ordering in the layers was revealed by TED performed on plan-view and cross-sectional samples prepared by standard methods. The (110) and $(\bar{1}10)$ cross sections were distinguished using convergent beam electron diffraction [13]. Extensive kinematic diffraction calculations were performed using the CrystalKit program to distinguish between different possible quadruple-period ordered structures. The ordered structure in Fig. 1(b) gives the best match to the experiment. These studies provide supports to this structure in additional to those given by high-resolution transmission electron microscopy, dynamical diffraction high-resolution TEM image simulations, and by quantitative synchrotron x-ray diffraction measurements [11].

Our calculations were carried out using the density functional theory under the local density approximation and a supercell approach. Ultrasoft pseudopotentials were used as implemented in the VASP code [14]. The supercell contains 12 atomic layers plus six equivalent vacuum layers, and the back surface of the slab was "passivated" by fractionally charged hydrogen atoms [15]. Except for the back surface, atoms are allowed to relax until the calculated forces are less than 0.02 eV/Å. For the study of the effects of dimer induced surface strain we kept the in-plane lattice constant at the calculated lattice constant of GaAs, 5.6 Å, which is less than 1% smaller than experiment. For other surface energy calculations the lattice constant of the alloy was kept to that expected by Vegard's law. A 150 eV cutoff energy was used in the calculation. Increasing the cutoff energy to 180 eV has little effect on the main results.

Before studying surface induced ordering, it is important to determine the surface reconstruction that is responsible for the ordering. The phase diagram of the Sb-stabilized GaAs(001) surfaces has been calculated by Schmidt and Bechstedt [16] revealing three stable structures in the order of decreasing Sb coverage: $\beta 2_3$, δ_2 (see Fig. 2), and δ_1. The $\beta 2_3$ structure is a Sb-dimer terminated version of the well-established and widely observed $\beta 2\ (2 \times 4)$ reconstruction of the GaAs (001) surface [17]. From our RHEED measurements it was, however, concluded that the QP ordering is not associated with the low-growth-temperature $\beta 2$ phase but with a high-growth-temperature, less anion-rich phase, namely, one of the δ structures. In this study, we will use the δ_2 phase [which is also termed the $\alpha 2(2 \times 4)$ phase by others] for the following four reasons: (a) the δ_2 phase occupies a much larger phase space than the δ_1 phase; (b) the transformation from $\beta 2_3$ to δ_2 only requires the removal of one Sb dimer, whereas to δ_1 requires additional steps involving Sb/As dimer exchange; (c) the δ_2 phase has been observed by experiments [18,19], and (d) Sb segregation to the surface always lowers the energy. Hence, unless there is a significant Sb deficiency, which is not the case during the growth of the GaAsSb alloy, a large portion of the lower dimers (in Fig. 2) should be occupied by Sb.

We have calculated the energetics of the surface segregation of Sb. Taking the energy for Sb at site $L1S1$ [Fig. 2(b)] to be 0.0 eV, the energies at site $L2S4$ and $L5S2$ (a bulklike site) are 0.54 and 1.21 eV per 2-Sb atoms, respectively. This trend is in line with Miedema's rule [20] that the element with the lowest enthalpy of formation of the elemental solid (262 kJ/mol for Sb and 303 kJ/mol for As) segregates to the surface. Cross-sectional scanning tunneling microscopy (STM) provides experimental evidence for the Sb segregation[21].

In search of the microscopic origin of the QP ordering, we have first followed the traditional approach and studied the effects of the subsurface strains due to surface dimerization. Namely, we calculate the energy of a single substitutional Sb atom at the various atomic sites in the third anion layer ($L3$) (Fig. 2). We found that the Sb atom prefers only the $L3S4^*$ (0.0 eV) and $L3S3^*$ (0.01 eV) sites, as all other sites are typically 0.2 eV higher in energy (see

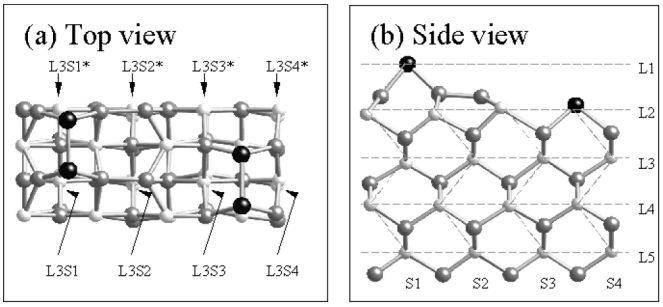

FIG. 2. Top and side views of the $\delta_2(2 \times 4)$ surface. Sb is black, As is small white, and Ga is large gray. The coordinates of the anion sites are indicated by the straight (horizontal) and zigzag (vertical) dashed lines, labeled as L_i and S_j.

TABLE I. Site preference energy (eV/Sb) in the $L3$ layer in Fig. 2, defined as the total energy difference of the various single-Sb configurations with respect to $L3S4^*$.

$L3S1^*$ ($L3S1$)	$L3S2^*$ ($L3S2$)	$L3S3^*$	$L3S3$	$L3S4^*$	$L3S4$
0.23	0.27	0.01	0.18	0.00	0.19

Table I). We also placed the Sb atom at the deeper ($L4$ and $L5$) layers and found that the energy difference between any two sites in a layer is insignificant as they are typically 1 order of magnitude smaller than the $L3$ layer. Although the subsurface strain model is consistent with the in-plane -As-As-Sb-Sb- arrangement in the QP structure (see Fig. 1), it is clear that the model provides no clue to the occurrence of the periodic antiphase boundaries, characteristic of the 3D ordering pattern.

In order to explain the antiphase boundary array, we noted that the Ga-Ga dimers at the topmost cation layer in Fig. 2 can be either to the left or to the right of the topmost ($L1$) Sb-Sb dimer via a flip-flop operation. During a layer-by-layer growth, for each added bilayer the topmost Ga-Ga dimers can change their positions with respect to the Sb-Sb dimers. If this flip-flop occurs in a regular fashion and if it is also coupled with Sb surface segregation, a periodic antiphase boundary can in principle result. To explore such a possibility, we have calculated the total energies for every possible combination of As and Sb atoms in the $L2$ layer, assuming a 50:50 As/Sb ratio. When the next bilayer is deposited, however, we assume that atoms in the buried, previous $L2$ layer cannot diffuse any further.

Figure 3 shows a sequence of the lowest-energy structures during layer-by-layer growth where the index for the key (k) second topmost anion layer changes from $k = L2$ to $k = L1$, $L0$, and L-1, respectively. Out of necessity, we will ignore the difference between the starred and unstarred sites in Fig. 2. Even so, there are still six inequivalent configurations for As/Sb in $k = L2$ due to the surface translational degree of freedom with respect to the substrate. There are 24 inequivalent configurations for $k = L1$ when the first GaAs(Sb) bilayer is added. There are 48 inequivalent configurations each for $k = L0$ and L-1 when the second and third bilayers are added. The numbers for $L0$ and L-1 are doubled with respect to $L1$ due to the flip-flop operation, which, however, adds no new state in either $L2$ or $L1$. These add up to 126 configurations, which are still too computationally intensive. By taking advantage of the Sb segregation into $L1S1$ ($L1S1^*$) and $L2S4$ ($L2S4^*$) sites [Fig. 3(a)] and into the subsequent equivalent sites in the $L0$, L-1, L-2 and $L1$, $L0$, L-1 layers, respectively, in Figs. 3(b)–3(d) during the growth, however, this number can be reduced to $3 + 12 + 24 + 24 = 63$. All of them have been calculated here.

For the three configurations in $k = L2$ we find that the lowest-energy structure [Fig. 3(a)] corresponds to Sb occupying $S3$ and $S4$ [denoted in Table II as ($S3$, $S4$)].

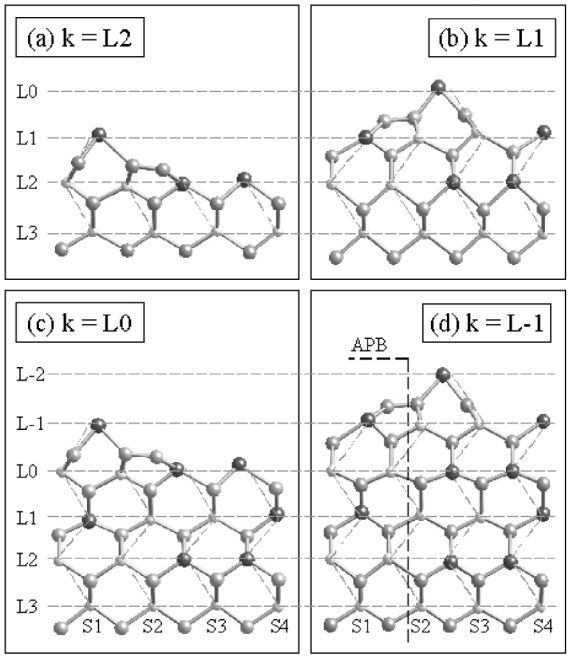

FIG. 3. Side view of ordered $GaAs_{0.5}Sb_{0.5}$ alloy during each step of the growth. The legends are the same as in Fig. 2. The thick dashed line is given to indicate the antiphase boundary (APB) observed by experiment in Fig. 1.

For the 12 configurations in $k = L1$, the ($S1$, $S4$) configuration in Fig. 3(b) has the lowest energy. For the 24 configurations in $k = L0$, the ($S3$, $S4$) configuration in Fig. 3(c) has the lowest energy. Finally, for the 24 configurations in $k = L$-1, the ($S1$, $S4$) configuration in Fig. 3(d) has the lowest energy. After four consecutive layer-by-layer growths, it is clear that the growth process will repeat itself. Note, however, that the resulting structure in Fig. 3(d) matches exactly with the experimentally determined pattern in Fig. 1(b).

There are several points worth mentioning. (i) Essential to our study, but long neglected in previous ordering models, is the mutual interaction between the already grown ordered substrate and the surface, i.e., a feedback effect. Without taking into account such an effect, we would also have missed the QP structure in Fig. 3(d). (ii) The ordering mechanism described here does not rely on preexisting surface steps. This is in agreement with our experiments on the QP ordering where the substrate orientation is singular. (iii) The QP structure

TABLE II. The calculated ground state, the next most stable state configurations, and the ordering energy (ΔE_{ord}), as a function of the key (k) layer during growth.

k layer	Ground state		Next state	
	Sb config.	(in Fig. 3)	Sb config.	ΔE_{ord} (eV)
$L2$	$S3$, $S4$	a	$S1$, $S4$	0.07
$L1$	$S1$, $S4$	b	$S2$, $S4$	0.22
$L0$	$S3$, $S4$	c	$S2$, $S4$	0.49
L-1	$S1$, $S4$	d	$S2$, $S4$	0.50

TABLE III. Calculated strain energy (meV/4-atoms) for alloys subject to periodicity constraints by surface reconstruction.

CuAu	$Y2$	$Y4$	QP	Random
89.6	77.5	102.2	74.6	80.4

obtained by the surface growth model is only partially consistent with the surface-dimerization induced 3rd anion layer strain model. (iv) Ordering occurs in a progressive fashion, defining the ordering energy ΔE_{ord} as the total energy difference between the next most stable state and the ground state in the k layer during epitaxial growth. Table II suggests that initially ΔE_{ord} is weak, 0.07 eV/cell. It increases with epilayer thickness and saturates at about 0.50 eV/cell after about four added bilayers. Grazing incidence x-ray diffraction [22] could be a way to test the proposed correlation between surface reconstruction and bulk ordering. In addition, since the model predicts that the topmost dimers in successive layers should flip-flop in a correlated fashion, an STM study looking for such a pattern on vicinal surfaces with monolayer height steps, coupled with ordering measurement, could provide a direct test of our model.

Finally, it is instructive to examine the quadruple-period ordering from bulk thermodynamics. Namely, what would be the lowest-energy bulk configuration with the constraints imposed by the reconstruction of the 2×4 surface? Neglecting the difference between the starred and unstarred sites in Fig. 2, there are only eight distinct bulk structures that form (110) superlattices and are commensurate with the (2×4) surface. These include the CuAu phase [a (1,1) superlattice], the $Y2$ phase [a (2,2) superlattice], the $Y4$ phase [a (4,4) superlattice], and the QP phase [a (2,1,1,2,1,1) superlattice]. We have performed valence-force-field calculations on these structures. Table III summarizes the results. For comparison, we also give the energy for the random alloy represented by an $SQS8$ model [23]. We find that the QP phase has the lowest (strain) energy among all the structures and is even lower in energy than the random alloy. Furthermore, if we assume that each of the (001) layers is made of the desirable -As-As-Sb-Sb- pattern along the [110] direction, then any stacking of the layers in the [001] direction will result in a polytype [24] with its strain energy between those of $Y4$ and QP (the two end-point compounds), i.e., the strain energy will always be higher than that of QP. This is in contrast to the CuPt-type ordering observed in most III-V semiconductor alloys where the ordered bulk structure has the highest strain energy. Hence, the QP ordering is also enhanced by its bulk stability due to its small strain energy.

In summary, a surface growth model was developed to explain the quadruple-period ordering found in MBE-grown GaAsSb alloys. The model reveals an important interaction between the substrate and the surface during layer-by-layer growth. In contrast to previous surface-dimerization and reconstruction induced ordering models that only produce 2D patterns, the surface growth model here is truly three dimensional in nature. Bulk calculations were also carried out. It was found that under certain surface constraints the calculated bulk strain energy is also in favor of the formation of the QP ordered structure.

It is a pleasure to acknowledge Sarah R. Kurtz for a critical reading of the manuscript. This work was supported by the U.S. DOE/BES under Contract No. DE-AC36-99GO10337 and NERSC for MPP time.

[1] *Spontaneous Ordering in Semiconductor Alloys*, edited by A. Mascarenhas (Kluwer, New York, 2002).
[2] J. E. Bernard *et al.*, Phys. Rev. B **38**, 6338 (1988).
[3] J. A. Appelbaum and D. R. Hamann, Surf. Sci. **74**, 21 (1978).
[4] P. C. Kelires and J. Tersoff, Phys. Rev. Lett. **63**, 1164 (1989).
[5] F. K. LeGoues *et al.*, Phys. Rev. Lett. **64**, 2038 (1990); J. E. Bernard, S. Froyen, and A. Zunger, Phys. Rev. B **44**, 11 178 (1991); B. A. Philips *et al.*, J. Cryst. Growth **140**, 249 (1994); S. B. Zhang, S. Froyen, and A. Zunger, Appl. Phys. Lett. **67**, 3141 (1995); S. Froyen and A. Zunger, Phys. Rev. B **53**, 4570 (1996).
[6] G. S. Chen and G. B. Stringfellow, Appl. Phys. Lett. **59**, 324 (1991).
[7] S. R. Kurtz *et al.*, J. Appl. Phys. **75**, 5110 (1994).
[8] A. Gomyo *et al.*, NEC Res. Develop. **35**, 134 (1994).
[9] J.-L. Li *et al.*, Phys. Rev. Lett. **88**, 066101 (2002); J. Jia *et al.*, Appl. Phys. Lett. **80**, 3186 (2002).
[10] A. G. Norman *et al.*, Inst. Phys. Conf. Ser. **134**, 279 (1993).
[11] Z. Zhong *et al.*, Phys. Rev. B **63**, 033314 (2001).
[12] C. Barrett and T. B. Massalski, *Structure of Metals* (Pergamon, Oxford, 1980), 3rd revised ed., Chap. 11.
[13] J. Tafto and J. C. H. Spence, J. Appl. Crystallogr. **15**, 60 (1982).
[14] G. Kresse and J. Hafner, Phys. Rev. B **47**, 558 (1993).
[15] K. Shiraishi, J. Phys. Soc. Jpn. **59**, 3455 (1990).
[16] W. G. Schmidt and F. Bechstedt, Phys. Rev. B **55**, 13 051 (1997).
[17] J. E. Northrup and S. Froyen, Phys. Rev. B **50**, 2015 (1994).
[18] P. Moriarty *et al.*, Phys. Rev. B **53**, R16 148 (1996).
[19] F. Maeda, Y. Watanabe, and M. Oshima, Phys. Rev. B **48**, 14 733 (1993).
[20] A. R. Miedema, Z. Metallkd. **69**, 455 (1978).
[21] J. Steinshnider *et al.*, Phys. Rev. Lett. **85**, 4562 (2000).
[22] M. Sauvage-Simkin *et al.*, Phys. Rev. Lett. **75**, 3485 (1995).
[23] A. Zunger *et al.*, Phys. Rev. Lett. **65**, 353 (1990).
[24] S. H. Wei, S. B. Zhang, and A. Zunger, Phys. Rev. B **59**, R2478 (1999).